Active Contour Model Based Object Contour Detection Using Genetic Algorithm with Wavelet Based Image Preprocessing

Kyeong-Jun Mun, Hyeon Tae Kang, Hwa-Seok Lee, Yoo-Sool Yoon, Chang-Moon Lee, and June Ho Park

Abstract: In this paper, we present a novel, rapid approach for the detection of brain tumors and deformity boundaries in medical images using a genetic algorithm with wavelet based preprocessing. The contour detection problem is formulated as an optimization process that seeks the contour of the object in a manner of minimizing an energy function based on an active contour model. The brain tumor segmentation contour, however, cannot be detected in case that a higher gradient intensity exists other than the interested brain tumor and deformities. Our method for discerning brain tumors and deformities from unwanted adjacent tissues is proposed. The proposed method can be used in medical image analysis because the exact contour of the brain tumor and deformities is followed by precise diagnosis of the deformities.

Keywords: Genetic algorithm, image preprocessing, object contour detection, wavelet.

1. INTRODUCTION

It is important to extract the interested region from the object in computer vision. Generally, there are two types of solution methods for this problem, a region based method and a contour extraction method. Several methods are proposed to extract the contour of an object such as hough transform, graph search, dynamic programming, region growing, etc. [1].

An active contour model was proposed by Kass, Witkin and Terzopoulos [2]. It constructs active contours to extract the contour of an object. By minimizing the energy it was applied to the low level vision problem [3]. Also, research is achieving much in the reflex analysis field of medicine because it is in agreement with the complex biological structure [2].

The active contour model, however, displays unstable behavior and contraction in the energy minimization process. When the contour of an object is incorrect then shock phenomenon of the active contour occurs. It structurally falls in the local minimum. Also, the conventional method has limitations in the case of initialization problems, robustness for noise and contour extraction of concaved shape objects. Cohen, William and Amini used an optimization algorithm such as the greedy algorithm dynamic problem to overcome these difficulties [4]. Recently, active contour is proposed considering the direction of edge [5] and genetic algorithm (GA) [6]. These methods, however, have difficulty in finding the contour of an object with a complex background and are time consuming.

In this paper, we propose an active contour model using GA with wavelet transform based image preprocessing to resolve the problems. Energy function is proposed to overcome vulnerability of the energy form that is presented in the existing method. We introduced the wavelet transform [7] and GA for selecting a search region. We outlined the contour of the interested object.

2. BASIC ACTIVE CONTOUR MODEL

In the active contour algorithm, selection of an energy function for extracting the contour of an object is important. Generally, energy function is composed of internal energy ($E_{\text{int}ernal}$), external energy (E_{ext}), and image energy (E_{image}) and is shown in (1) [1].

$$E_{snake} = \int_{s=0}^{1} [E_{\text{int}ernal}(v(s)) + E_{ext}(v(s)) + E_{image}(v(s))]\, ds\,, \quad (1)$$

Manuscript received March 12, 2003; revised January 15, 2004; accepted January 16, 2004. Recommended by Editorial Board member Sun Kook Yoo under the direction of Editor Jin Bae Park.

K. Mun, Y. Yoon, J. H. Park, and C. Lee are with the School of Electrical Engineering, Pusan National University, san 30 Jangjeon-dong, Keumjung-gu, Pusan 609-735, Korea (e-mail: {kjmun, locus5, jhpark}@pusan.ac.kr, mooni569@hanmail.net).

H. T. Kang is with the Korea Hydro and Nuclear Power, Uljin-gun, Kyeongbuk, 767-701, Korea (e-mail: isaiah@pusan.ac.kr).

H. Lee is with the School of Electrical Engineering, Koje College, 654-1 Jangsungpo-dong, Koje, Kyongnam 656-701, Korea (e-mail: hslee@koje.ac.kr).

where E_{snake} : Total energy,
$v(s)$: Control point,
s : Distance between control points.

In (1), internal energy is shown in (2). In (2), the first derivative term is approximated by a finite difference, which makes a snake-like smoothed curve, and the second derivative term makes a snake-like straight line. Changeable weighting parameters $\alpha(s)$, $\beta(s)$ control the contour of the snake freely so that we can obtain the accurate shape contour [1].

$$E_{\text{int}ernal} = \frac{1}{2}\left(\alpha(s)\left|\frac{\partial v(s)}{\partial s}\right|^2 + \beta(s)\left|\frac{\partial^2 v(s)}{\partial s^2}\right|^2 \right) \quad (2)$$

Image energy is shown as in (3). The snake shape is moved toward the direction of maximum image gradient intensity. External energy is constraint by user [1].

$$E_{image} = -\gamma\left|\nabla I(x,y)\right|^2 , \quad (3)$$

where γ : Weight of image energy.

3. WAVELET TRANSFORM

3.1. Concept

The Fourier transform analyses the frequency contents of a signal. Its many properties make it suitable for studying linear time invariant operators, such as differentiation. As shown in (4), however, to represent the frequency behavior of a signal locally in time domain, the signal should be analyzed by functions that are localized both in time and frequency domain, which is called Short Time Fourier Transform (STFT). For instance, signals are compactly supported in the time and frequency domains. STFT for $s(t)$ is shown below [7].

$$STFT(t', f) = \int_{-\infty}^{\infty}[s(t)\cdot w(t-t')]\cdot e^{-iwt}dt , \quad (4)$$

where t' : Shifted time,
$w(t)$: Window function,
e^{-iwt} : Sinusoidal wave,
$s(t)$: Time signal.

The wavelet transform replaces the Fourier transforms sinusoidal waves by a family generated by translations and dilations of a window known as a wavelet. Wavelet function ($\psi_{a,b}(t)$) is the fundamental function used to transform the mother wavelet. It is shown in (5).

$$\psi_{a,b}(t) = \frac{1}{\sqrt{a}}\psi\left(\frac{t-b}{a}\right) , \quad (5)$$

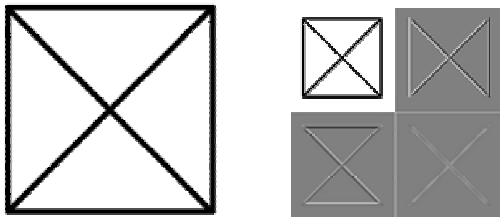

Fig. 1. 2D decomposition.

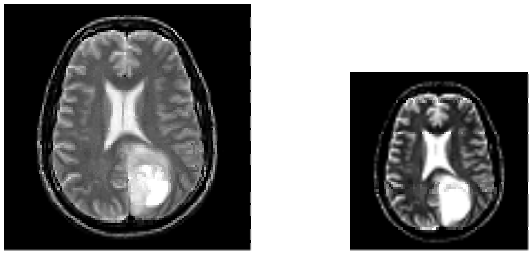

(a) Original image. (b) Coarse image.

Fig. 2. 2D multi-resolution image.

where a : Dilation,
b : Translation.

Wavelet transform ($CWT_s(a,b)$) for $s(t)$ using wavelet is shown in (6). The wavelet transform is a correlation of original signal and wavelet function. $CWT_s(a,b)$ represents a signal into several resolutions according to a and b.

$$CWT_s(a,b) = \langle \psi_{a,b}(t), s(t) \rangle = \frac{1}{\sqrt{a}}\int_{-\infty}^{\infty}\psi\left(\frac{t-b}{a}\right)s(t)dt \quad (6)$$

3.2. 2D Wavelet transform

The fundamental module from which the DWT is composed is a “perfect reconstruction two-channel filter bank [7]”, which applies a low pass filter (which attenuates high frequencies) to one channel, and a high pass filter (which attenuates low frequencies) to the other. These modules are cascaded on the low pass channel, the output of which is fed into the next module, while the output of the high pass channel is a representation of one level of the detail information added to create representations of increasing resolution. The figure below represents one-level wavelet decomposition, constructed as a cascade of a two-channel filter bank. 2D decomposition is obtained by applying the one-dimensional decomposition to the image rows and columns as shown in Fig. 1.

4. ACTIVE CONTOUR MODEL USING GA WITH WAVELET BASED IMAGE PREPROCESSING

4.1. Image preprocessing

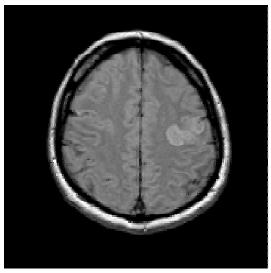

(a) Vague boundary.

(b) Clear boundary after DWT.

Fig. 3. Image preprocessing on vague boundary between the region of interest and its adjacent background.

Image energy uses an approximated image obtained by the discrete wavelet transform (DWT) of original image. For example, Fig. 2 shows the multi-resolution analysis of the original image. One coarse image is generated by DWT. Detailed images are not shown. The coarse image is used in detecting the contour of an object as shown in Fig. 2 (b).

Because the energy of the coarse image by DWT is reserved by the characteristics of DWT, the intensity of the image according to resolution is different. In this paper, if the gray level is larger than a set point, as the scaling of a coarse image by DWT is higher, the intensity of the transformed image is higher. However, if the gray level of the original image is lower than the set point, the opposite holds true. Therefore, if the border between the interested region and background region is vague (Fig. 3), use of the higher scaled image helps the border to be clear.

4.2. Energy of active contour model

In this paper, we proposed a genetic algorithm for the optimization process, precise object contour detection with wavelet based preprocessing to detect the contour of object effectively. The energy function using the proposed method is composed of internal energy, which means continuity energy, curvature energy, and image energy. Each of the energy terms are shown below.

4.2.1 Internal energy

Continuity and curvature energy are scale-invariant. When an active contour is modeled as spline, continuity energy is shown in (7) and curvature energy is shown in (8). In curvature terms, in the case of 90° curvature, this energy is 0.5.

$$E_{continuity}(v_i) = (\bar{L} - |u_i|)^2 / \bar{L}^2, \tag{7}$$

$$E_{curvature}(v_i) = \frac{1}{4}\left|\frac{u_i}{|u_i|} - \frac{u_{i-1}}{|u_{i-1}|}\right|, \tag{8}$$

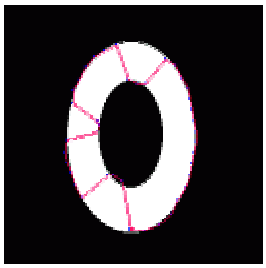

Fig. 4. Edge detection using edge gradient magnitude only.

where $\bar{L} = \frac{1}{N}\sum_{i=1}^{N}|u_i|$: Euclidean distance of control points v_i : $i-th$ control point $u_i = v_{i+1} - v_i$.

4.2.2 Image energy

As generally used image energy considers the magnitude of image gradient energy ($|\nabla I(x,y)|$), it is difficult to detect the contour of the interested region with a complex background. In this paper, therefore, the gradient magnitude and directional information of the image was considered. It is shown in (9) and (10).

$$|\nabla I(x,y)| = \sqrt{G_x(x,y)^2 + G_y(x,y)^2}, \tag{9}$$

$$\theta_G(x,y) = \tan^{-1}\left(\frac{G_y(x,y)}{G_x(x,y)}\right), \tag{10}$$

where $I(x,y)$: gray level in (x,y)

$G_x(x,y) = I(x,y) * M_x(x,y)$: edge gradient of x direction

$G_y(x,y) = I(x,y) * M_y(x,y)$: edge gradient of y direction

$M_x(x,y), M_y(x,y)$: horizontal and vertical gradient mask.

Fig. 4 shows the contour of an object, which is detected only by using the gradient magnitude of the image. As shown in Fig. 4, because the magnitude of the gradient intensity of the image is considered, in an object with unwanted edge gradient direction, the interested edge is not detected. Fig. 5 however, shows that both the magnitude and the edge gradient direction of the image are considered, as a new trend in image processing. As shown in Fig. 5, considering all images, the interested edge was detected according to the outer and inner edge gradient direction.

Therefore in this paper, image energy ($E_{image}(v_i)$) was shown as considering the direction of the active contour. In (11) the direction of image energy was weighted strongly by $\cos\delta(v_i)$ [5]. Furthermore, the value of the gradient magnitude of image energy is

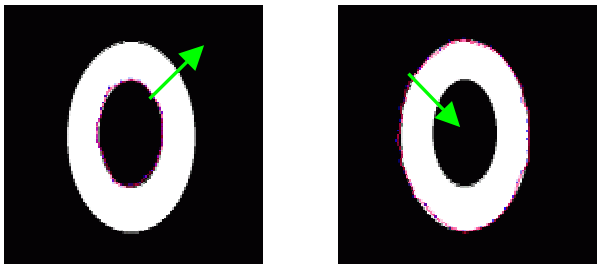

(a) Outward edge gradient direction. (b) Inward edge gradient direction.

Fig. 5. Edge detection using edge gradient direction.

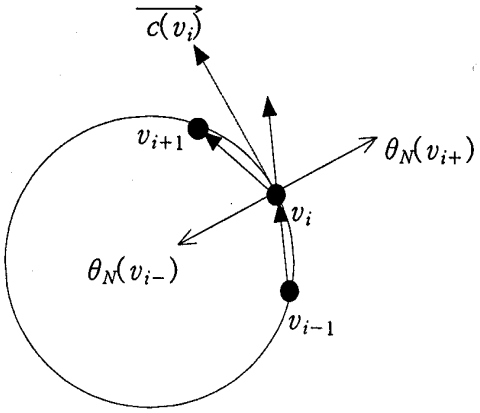

Fig. 6. Tangential and normal vectors of active contour.

between 0 and 255. The value is normalized [0 1] using (12).

$$E_{image}(v_i)=\begin{cases}1-\left|\nabla I(v_i)\right|\left|\cos\delta(v_i)\right|, if\ \left|\delta(v_i)\right|<\dfrac{\pi}{2}\\ 1, \qquad otherwise\end{cases} \tag{11}$$

$$\nabla I(v_i)=\frac{g_{\max}-g_{v_i}}{g_{\max}-g_{\min}}, \tag{12}$$

where g_{v_i} : Gradient magnitude in v_i $g_{\max}, g_{\min}$: Maximum and minimum gradient magnitude of contour point.

Fig. 6 shows the active contour model considering edge gradient direction. As shown in Fig. 6, $\theta_G(v_i)$ is the gradient direction in v_i. $\theta_N(v_i)$ is the normal direction in v_i. When $\overrightarrow{c_{(v_i)}}$ is the directional vector of the active contour in v_i, (13) is possible. Supposing $\overrightarrow{c_{(v_i)}}=(c_x,c_y)$, as shown in (14), the normal vector is found. $\theta_N(v_{i+})$ and $\theta_N(v_{i-})$ are selected properly according to $\theta_G(v_i)$.

$$\overrightarrow{c(v_i)}=\overrightarrow{v_iv_{i+1}}+\overrightarrow{v_{i-1}v_i} \tag{13}$$

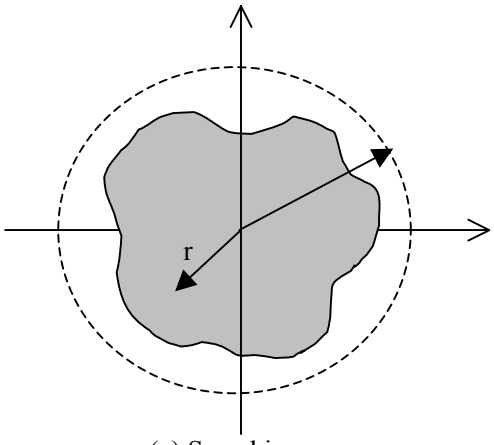

(a) Searching range.

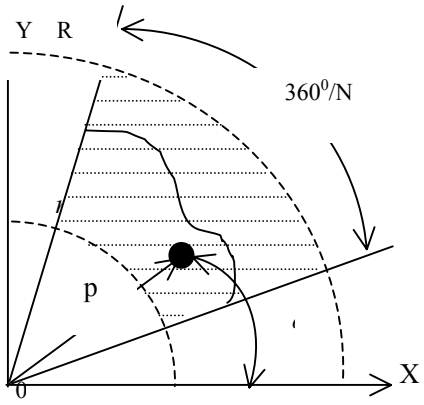

(b) Exclusive searching range.

Fig. 7. Searching region.

$$\theta_N(v_{i\pm})=\tan^{-1}(\frac{c_y}{c_x})\pm\frac{\pi}{2} \tag{14}$$

4.3. Active contour model using GA

The most important aspect concerning application of an active contour model using GA is to select the appropriate population and fitness function. Selecting proper population saves searching time in the optimization process and selecting proper fitness function lessens the convergence time. The searching region should be decided for detecting the contour of the object using GA. Fig. 7 shows the searching region for detecting the contour of an object using GA.

In this paper, therefore, the population is constructed using the distance and angle from the center to the control point as shown in Fig. 8. The fitness function for evaluating each string is composed of image energy, continuity energy and curvature energy in (15). The fitness will be a maximum if energies are minimal.

$$Fitness=\frac{1}{1+(\gamma E_{image}+\alpha E_{continuity}+\beta E_{curvature})} \tag{15}$$

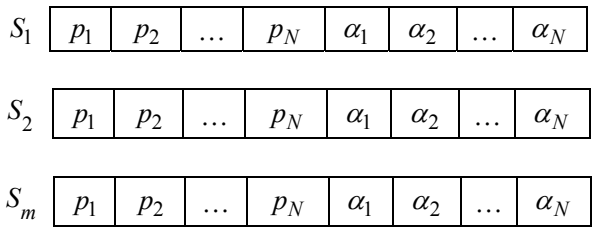

where N : number of control point,
p_i $(i = 1, \cdots, N)$: Distance from center of object to control point,
α_i $(i = 1, \cdots, N)$: Angle crossing control point and x axis,
m : number of population.

Fig. 8. String architecture.

5. SIMULATION RESULTS

We accomplished the computer simulation for detecting the contour of the interested region to prove the efficiency of the proposed method. Fig. 9 shows the fitness of GA. As shown in Fig. 9 the fitness improves as generation evolves, which means the spline is optimized by GA and close to the contour of the object. The control points for detecting the contour of the object are 60, which are initially set randomly within the searching range by GA operation. Table 1 shows the simulation coefficients of GA. Fig. 9 shows a rapid convergence to the optimal solution compared to the over 10000 generation of the paper by L. Ballerini [6], which does not use wavelet based image preprocessing.

To improve the efficiency of the proposed method as shown in Fig. 10, adding 40% and 60% gaussian noise into the synthesized image, we accomplished computer simulation. The contour of the interested region was detected without being affected by the added noise.

Using (11) and uniformed intensity of an object preprocessed by wavelet transform [7], the interested region of an image with complex background was outlined. Fig. 11 shows the detection of the interested region using the proposed GA in case that the higher gradient intensity exists other than in the region of interest. The contour of an object was detected by the

Table 1. Simulation coefficients of GA.

Number of population	Generation		Crossover rate
100	150		0.65
Mutation rate	Coefficients of fitness		
0.01	α	β	γ
	1.2	0.1	0.1

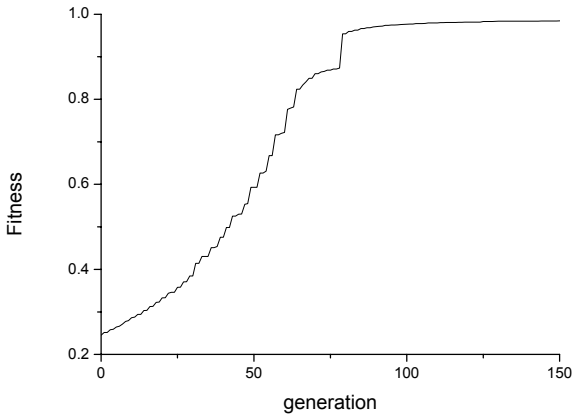

Fig. 9. Fitness.

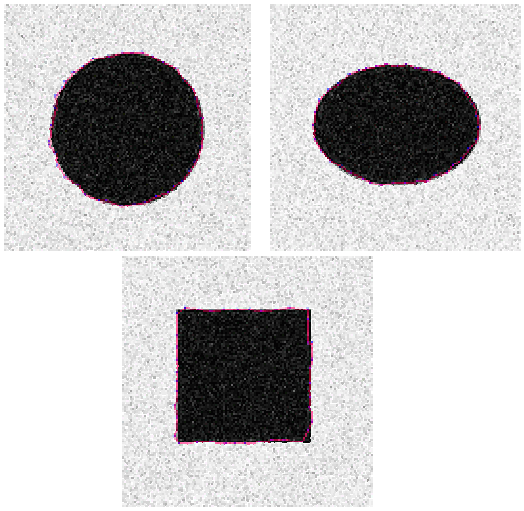

(a) 40% gaussian noise added image.

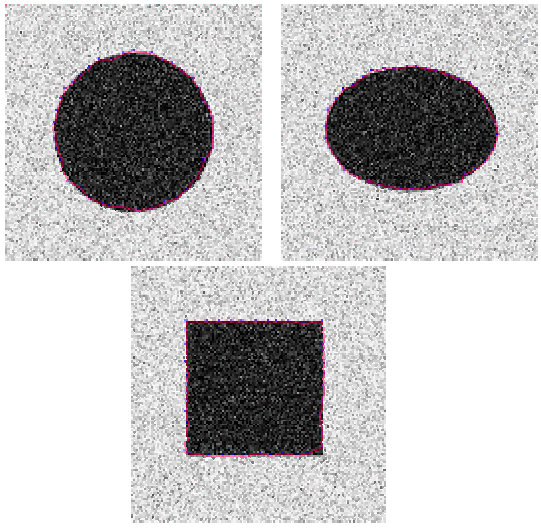

(b) 60% gaussian noise added image.

Fig. 10. Examples of synthesized images with differentvalues of Gaussian noise.

(a) Coin image.

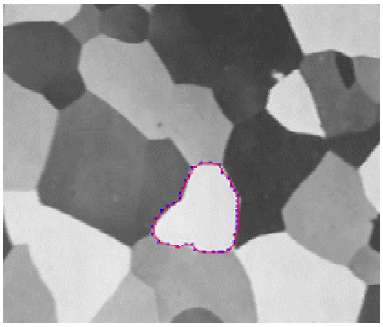

(b) Metal image.

Fig. 11. Detection of contour of some objects.

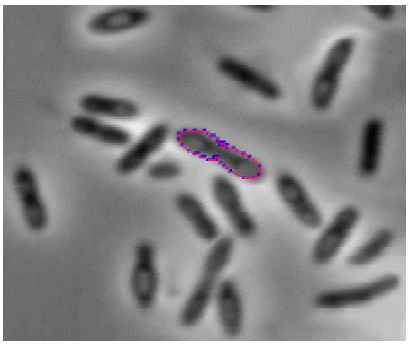

(a) Bacteria

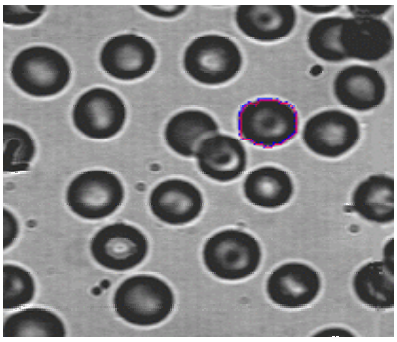

(b) Blood.

Fig. 12. Detection of contour of bacteria and blood image.

proposed method accurately. Also, as shown in Fig. 12, we accomplished detection of the contour of the bacteria and blood image to show the efficiency of the proposed method.

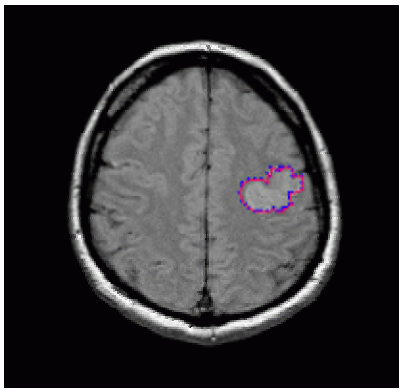

(a) Brain attack.

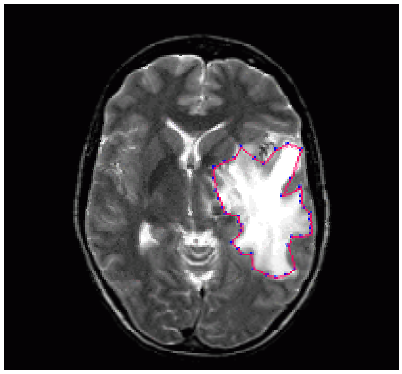

(b) Brain tumor.

Fig. 13. Detection of contour of fatal attack and brain tumor.

Fig. 13(a) shows that when the border of brain attack and its adjacent sound tissue is not distinct, the contour of the interested region could be detected accurately. To illustrate the efficiency of the proposed method, the contour of the brain tumor was detected to be unaffected by its other complex sound tissue.

6. CONCLUSIONS

In this paper, we presented a novel, rapid approach for contour detection of the region of interest in complex background images using a genetic algorithm with wavelet based preprocessing. The contour detection problem is formulated as an optimization process that seeks the outline to minimize an energy function based on an active contour model. The object contour, however, cannot be detected in cases in which the higher gradient intensity exists other than in the region of interest. We've proposed a method to solve the problem for discerning the region of interest from unwanted regions in complex background images using the directional information of an object's edge. The proposed method can be used in medical image analysis because the exact contour of the brain tumor and deformities is followed by precise diagnosis of the deformities.

REFERENCES

[1] D. H. Ballard, *Christopher M. Brown, Computer Vision*, Prentice-hall, 1982.

[2] R. Baldock and J. Graham, *Image Processing and Analysis – A Practical Approach*, Oxford University Press, 2000.

[3] A. Blake and M. Isard, *Active Contours - The Application of Techniques from Graphics, Vision, Control Theory and Statistics to Visual Tracking of Shape in Motion*, Springer-Verlag, 2000.

[4] D. J. Willams and M. Shah, "Fast Algorithm for Active Contours and Curvature Estimation," *Computer Vision, Graphic, and Image Processing*, vol. 55, no. 1, pp. 14-26, 1992.

[5] D. Tim and P. Plassmann, "An active contour model for measuring the area of leg ulcers," *IEEE Trans. on Medical Imaging*, vol. 19, no. 12, pp. 1202-1210, December 2000.

[6] L. Ballerini, "Genetic snakes for medical images segmentation," *Proc. of first European Workshop on Evolutionary Computation in Image Analysis and Signal Processing*, Goteborg, Sweden, May 1999.

[7] I. Daubechies, *Ten Lectures on Wavelets*, SIAM, 1992.

Kyeong-Jun Mun received the B.S. and M.S. degrees in Electrical Engineering from Pusan National University in 1994 and 1996. His research interests include applications of intelligent systems and distribution automation.

Hyeon Tae Kang received the B.S. and M.S. degrees in Electrical Engineering from Dong-A University and Pusan National University in 1998 and 2002, respectively. He is currently a Nuclear System Engineer at Korea Hydro and Nuclear Power in Uljin, Korea. His research interests include computer vision and signal processing.

Hwa-Seok Lee received the B.S., M.S., and Ph.D. degrees in Electrical Engineering from Pusan National University in 1991, 1993, and 1997 respectively. He is currently an Assistant Professor at Koje College. His research interests include power quality, intelligent systems, and distribution automation.

Yoo-Sool Yoon received the B.S. degree in Electrical Engineering from Dong-A University in 1999. He is currently taking pursuing his M.S. at Pusan National University.

Chang-Moon Lee received the B.S. and M.S. degrees in Electrical Engineering from Pusan National University in 2001 and 2003. He is currently an Engineer at the Korea Electric Power Corporation.

June Ho Park received the B.S., M.S., and Ph.D. degrees from Seoul National University, in 1978, 1980 and 1987, respectively, all in Electrical Engineering. He is currently a Professor at Pusan National University. His areas of interest are intelligent systems applications to power systems. Dr. Park has been a member of the IEEE Power Engineering Society, Control System Society, and Systems Man and Cybernetics Society.